New Phytologist

Spatial distribution of arsenic and temporal variation of its concentration in rice

Mao-Zhong Zheng[1], Chao Cai[1], Ying Hu[2], Guo-Xin Sun[2], Paul N. Williams[3], Hao-Jie Cui[1], Gang Li[1], Fang-Jie Zhao[4] and Yong-Guan Zhu[1,2]

[1]Key Laboratory of Urban Environment and Health, Institute of Urban Environment, Chinese Academy of Science, Xiamen 361021, China; [2]Research Center for Eco-Environmental Sciences, Chinese Academy of Sciences, Beijing 100085, China; [3]Lancaster Environment Centre, Lancaster University, Lancaster LA1 4YQ, UK; [4]Soil Science Department, Rothamsted Research, Harpenden, Hertfordshire AL5 2JQ, UK

Author for correspondence:
Yong-Guan Zhu
Tel: +86 10 62936940
Email: ygzhu@rcees.ac.cn

Received: *12 June 2010*
Accepted: *9 August 2010*

New Phytologist (2011) **189**: 200–209
doi: 10.1111/j.1469-8137.2010.03456.x

Key words: arsenic (As), grain filling, rice (*Oryza sativa*), speciation, translocation.

Summary

• In order to gain insights into the transport and distribution of arsenic (As) in intact rice (*Oryza sativa*) plants and its unloading into the rice grain, we investigated the spatial distribution of As and the temporal variation of As concentration in whole rice plants at different growth stages. To the best of our knowledge, this is the first time that such a study has been performed.

• Inductively coupled plasma mass spectroscopy (ICP-MS) and high-performance liquid chromatography (HPLC)-ICP-MS were used to analyze total As concentration and speciation. Moreover, synchrotron-based X-ray fluorescence (SXRF) was used to investigate *in situ* As distribution in the leaf, internode, node and grain.

• Total As concentrations of vegetative tissues increased during the 2 wk after flowering. The concentration of dimethylarsinic acid (DMA) in the caryopsis decreased progressively with its development, whereas inorganic As concentration remained stable. The ratios of As content between neighboring leaves or between neighboring internodes were *c*. 0.6. SXRF revealed As accumulation in the center of the caryopsis during its early development and then in the ovular vascular trace.

• These results indicate that there are different controls on the unloading of inorganic As and DMA; the latter accumulated mainly in the caryopsis before flowering, whereas inorganic As was mainly transported into the caryopsis during grain filling. Moreover, nodes appeared to serve as a check-point in As distribution in rice shoots.

Introduction

Inorganic arsenic (As) is a well-known class 1, nonthreshold carcinogen (Smith *et al.*, 2002). In recent decades, As accumulation in the soil in some parts of the world has increased dramatically as a result of mining (Liao *et al.*, 2005; Zhu *et al.*, 2008), irrigation with As-contaminated groundwater (Meharg & Rahman, 2003; Williams *et al.*, 2006) and the use of arsenical pesticides (Williams *et al.*, 2007). Elevated As accumulation in drinking water is affecting millions of people directly in Bangladesh and West Bengal, India (Bhattacharjee, 2007). Recent studies have indicated that rice (*Oryza sativa*) is an important source of inorganic As for populations dependent on a rice diet (Kile *et al.*, 2007; Ohno *et al.*, 2007; Mondal & Polya, 2008), as a consequence of the high efficiency of rice in accumulating As (Meharg *et al.*, 2008; Sun *et al.*, 2008; Williams *et al.*, 2009; Zhao *et al.*, 2010). Furthermore, human exposure to As may result from the uses of harvested residues, such as straw, husk and bran, as fertilizers, animal feed, building materials and fuel. Therefore, the uptake, metabolism, transport and accumulation of As in rice have received considerable attention.

Arsenic accumulation in rice is determined by many factors, such as soil conditions, the uptake capacity of roots, the efficiency of translocation, and the distribution and redistribution of As among plant tissues. Several studies have shown that arsenate (As(V)), arsenite (As(III)), dimethylarsinic acid (DMA) and monomethylarsonic acid (MMA) are present in rice vegetative tissues and grains (Abedin *et al.*, 2002; Williams *et al.*, 2005; Zhu *et al.*, 2008). These As species and their concentrations in rice

were found to vary with soil conditions, rice cultivar and soil moisture regime (Xu *et al.*, 2008; Arao *et al.*, 2009; Li *et al.*, 2009; Norton *et al.*, 2010a). As(V), the predominant form of As in aerobic soils, is an analog of phosphate and shares the same transport pathway with phosphate in the rice root (Abedin *et al.*, 2002). As(III) dominates in anaerobic environments and is taken up by rice roots via silicic acid transporters (Ma *et al.*, 2008). The uptake of methylated species (DMA and MMA) by rice plants, although much slower than that of inorganic As, is also partly mediated by the silicic acid transporter Lsi1 (Li *et al.*, 2009). Once taken up, As(V) is reduced to As(III) by arsenate reductases (Duan *et al.*, 2005), and then may be complexed with glutathione or phytochelatins followed by sequestration in the vacuole (Bleeker *et al.*, 2006; Zhao *et al.*, 2009; Liu *et al.*, 2010), or enter the xylem via a silicic acid/arsenite effluxer (Ma *et al.*, 2008). Although knowledge of As uptake by the plant root has developed rapidly (Zhao *et al.*, 2009), there is little information about how As is translocated within rice plants after its absorption by roots.

To expand our knowledge of As transport and accumulation in intact rice plants, and its unloading into the rice grain, we present here for the first time a study investigating the variation of As concentration and speciation in different plant tissues throughout the growth period of rice. Total As concentrations in roots, leaves, internodes, husks and grains were quantified by inductively coupled plasma mass spectroscopy (ICP-MS) and As speciation was determined using high-performance liquid chromatography (HPLC)-ICP-MS. Moreover, synchrotron-based X-ray fluorescence (SXRF) was used to map the As localization patterns in the leaf, internode, node and grain, providing further insights into the mechanism underlining the transport and accumulation of As in the grain.

Materials and Methods

Plant culture and sample collection

Pot experiments were performed in a glasshouse at ambient temperatures (14–38°C) under sunlight, in Xiamen, China. Uncontaminated soil was collected from the plow layer of a paddy rice field, air-dried, sieved to < 8 mm, and homogenized. In order to avoid As toxicity and ensure normal growth of the rice plant, relatively low doses of As and basal fertilizers (10 mg As kg^{-1} soil as $Na_3AsO_4{\cdot}12H_2O$, 65 mg phosphorus (P) kg^{-1} soil as $CaH_2PO_4{\cdot}H_2O$, 166 mg potassium (K) kg^{-1} soil as KCl, and 200 mg nitrogen (N) kg^{-1} soil as $CO(NH_2)_2$) were added to the soil and mixed in thoroughly.

One hundred and twenty seedlings of rice (*Oryza sativa* L., cv Zhe-704) were germinated on perlite and transplanted into the soil on 5 May 2009, with 4 kg soil and two rice seedlings per 4-l PVC pot, and 2–3 cm of standing water was maintained. Of these rice plants, only 43 plants which flowered on the same day were used for analyses. According to the growth stage of the main tiller, four rice plants grown in different pots were harvested for each experiment at seven stages: (1) 38 d after transplant (DAT), when the rice plant was at the tillering stage; (2) 49 DAT, when the rice plant was at the booting stage; (3) 56 DAT, when the rice plant started to flower (0 d after flowering (DAF)); (4) 62 DAT, when the rice plant was at 6 DAF; (5) 69 DAT (= 13 DAF); (6) 76 DAT (= 20 DAF); and (7) 84 DAT (= 28 DAF), when the grain was mature. To avoid variation among tillers differing in their stage of development, the main tillers of above-ground tissues and all roots were used in this study. Plants were washed with deionized water and separated into husks, caryopses, pedicels, peduncles, internodes and leaves, which were numbered sequentially from top to bottom (Supporting Information Fig. S1). These tissues were blotted and dried in an oven overnight at 70°C to constant weight.

Analysis of total As

To remove iron plaques and the adsorbed As from the root surface, excised rice roots (2.1–9.0 g FW) were incubated in 50 ml of dithionite-citrate-bicarbonate solution (containing 0.03 M $Na_3C_6H_5O_7{\cdot}2H_2O$, 0.125 M $NaHCO_3$ and 0.06 M $Na_2S_2O_4$) for 1 h at room temperature (Chen *et al.*, 2005). After incubation the roots were oven-dried at 70°C to constant weight and ground. The method for determining total As concentrations has been described previously (Sun *et al.*, 2008). Four certified reference materials (CRMs), GBW10010 Chinese rice flour samples, four spikes and four blanks were used for quality control. Samples of 0.2 g were predigested overnight in 2 ml of concentrated nitric acid at room temperature, and were then digested in a microwave oven (MARS; CEM Microwave Technology Ltd, Matthews, NC, USA) on a three-stage temperature-ramping program. After digestion, 0.5 ml of 10 μg indium l^{-1} in 1% HNO_3 was added as an internal standard, and the digest was diluted to 50 ml with Millipore ultrapure water (Millipore, Billerica, MA, USA). Total As concentrations were determined using ICP-MS (Agilent 7500; Agilent Technologies, Palo Alto, CA, USA). In addition to m/z 75 (for As) and 115 (for indium), m/z 77, 78 and 82 were also measured to monitor polyatomic argon chloride interference; no polyatomic interference was detected. Mean As recovery from the rice flour CRM was 93.7 ± 1.0% (n = 4).

Determination of As species

For the analysis of As species, samples were powdered; 0.2 g was weighed into a 50-ml polyethylene centrifuge tube, and extracted with 10 ml of 1% nitric acid as described by Zhu

et al. (2008). The extraction solutions were centrifuged and passed through a 0.45-μm nylon filter. To minimize potential further transformation of As species, samples were kept on ice and in the dark and analyzed within a few hours after extraction. Arsenic species in the extracts were assayed by HPLC-ICP-MS (7500; Agilent Technologies). Chromatographic columns consisted of a Hamilton precolumn (length 11.2 mm, particle size 12–20 μm) and a Hamilton PRP-X100 10-μm anion-exchange column (240 × 4.1 mm) (Hamilton, Reno, Nevada, USA). The mobile phase consisted of 6.66 mM NH_4NO_3 and 6.66 mM $NH_4H_2PO_4$ (pH 6.2), and was run isocratically at 1 ml min^{-1}. Standard compounds of As(V), As(III), DMA and MMA were used to obtain retention times. Matrix-matched DMA standards were used to calibrate the instrument. Arsenic species in samples were identified by comparisons with the retention times of the standard compounds and quantified using external calibration curves with peak areas. Mean As recovery from the rice CRM was 77.1 ± 1.0% (n = 4).

In situ analyses using a synchrotron X-ray fluorescence (SXRF) microprobe

SXRF microprobe experiments were performed at beamline LU15 at the Shanghai Institute of Applied Physics, Chinese Academy of Science. Incident X-rays of 8.1 keV were used to excite elements of liquid nitrogen-frozen samples of leaf, internode, node and ovary or dehusked grain, which had been placed in liquid nitrogen immediately after cutting from the live plant. The SXRF signals were collected for up to 30 s for each point with a silicon (lithium) (Si (Li)) detector, using a spot size of 120 μm and step sizes ranging from 100 to 120 μm depending on the size of the area mapped. The fluorescence intensities of calcium (Ca), manganese (Mn), iron (Fe), copper (Cu), zinc (Zn), As and Compton scattering were recorded and analyzed using eight single channel analyzers (Vortex-Ex; SII Nano Technology, Northridge, CA, USA), respectively. In order to correct for the effect of synchrotron radiation beam flux variation on signal intensity, the fluorescence intensity was normalized to the incident X-ray intensity, which was monitored using an ionization chamber located in front of the K-B mirror modulating the size of beam. The corrected fluorescence intensity was used to estimate the relative elemental content.

Dye loading into the ovular vascular trace

To observe the ovular vascular trace in the developing grain, rice panicles at 10 d post anthesis were excised by cutting the pedicel under water. The excised panicles were immediately transferred to a 50-ml tube containing 40 ml of 6 mM aniline blue (prepared with deionized water) and incubated overnight at room temperature (Krishnan & Dayanandan, 2003). Grains were removed and washed with deionized water, and caryopses were separated and photographed under a dissecting microscope.

Results

Biomasses of various tissues during the development of rice plants

Fig. 1 shows changes in the biomasses of various tissues. Rice plants began to flower at 56 DAT, when leaf biomass reached its maximum and was maintained at a steady level until 84 DAT (Fig. 1a). By contrast, the biomass of internodes continued to increase up to 62 DAT, after which it was also maintained at a steady level (Fig. 1b). The biomass of the husk increased significantly after flowering, concomitant with a sharp increase in root DW. Interestingly, although the size of the caryopsis increased during the first week after flowering (Fig. S2), its dry weight did not increase; after 62 DAT, a dramatic increase in biomass was

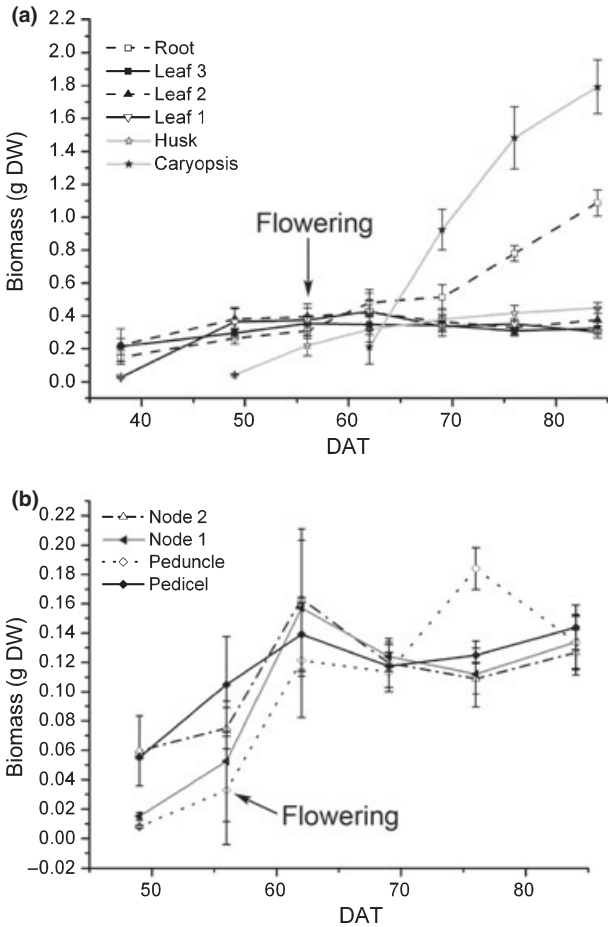

Fig. 1 Biomass (dry weights) of various tissues of rice (*Oryza sativa*) plants on different days after transplant (DAT). Plants were grown in a paddy soil amended with 10 mg As kg^{-1} soil as Na_3AsO_4. Data are the mean ± SE (n = 4).

observed in the caryopsis, suggesting that grain filling started at 62 DAT, 1 wk after flowering (Fig. 1a).

Arsenic distribution during the development of rice plants

The same samples as used in biomass measurements were used to quantify As concentrations; total As concentrations are plotted against DAT in Fig. 2. The As concentrations of roots decreased with growth stage, declining by 83.5% from 38 to 84 DAT (Fig. 2a). By contrast, As concentrations in leaves and internodes increased 2–3-fold after flowering to reach a peak at 69 or 76 DAT, after which they decreased by *c.* 50–85% (Fig. 2b,c). The As concentration in the pedicel showed the largest increase, from 0.51 ± 0.07 mg kg^{-1} DW at 49 DAT to 2.60 ± 0.18 mg kg^{-1} DW at 76 DAT, representing a *c.* 5-fold increase (Fig. 2c). Arsenic concentrations in the husk and caryopsis showed a similar trend to As concentrations in above-ground tissues, although the scale of changes was smaller (Fig. 2d). The As concentration in the caryopsis showed only a small increase (13.3%) from 62 to 69 DAT, after which it decreased again, declining by 26.5% from 69 to 84 DAT. Generally, Fig. 2 also reveals that plant parts ranked in terms of total As concentration as follows: iron plaque > root > leaf 3 > leaf 2 > internode 2 > leaf 1 > pedicel > internode 1 > peduncle > husk > caryopsis. It is worthy of note that the pedicel, the tissue that supports the rice flowers and spikelet (Fig. S1), contained a higher concentration of As than internode 1 and the peduncle.

Arsenic contents in various above-ground tissues of the main tiller and entire root were calculated by multiplying As concentrations by the corresponding biomass (Fig. 3). The root As content showed a 33.2% decrease before flowering (from 38 to 56 DAT), after which it increased 1.24-fold in the following 20 d until 76 DAT, to give a final reduction of 19.7%; this pattern was similar to that for the As concentration in the root, but the variations were of a different magnitude (Fig. 3a compared with Fig. 2b). The trends for As contents in the leaves, internodes, peduncles and pedicels were more similar to those for As concentrations than to those for biomass, whereas in the husk and caryopsis the As contents increased with biomass (Fig. 3b,c compared with Figs 1 and 2c). Furthermore, increases in the As contents of the above-ground tissues coincided with increases in the As content of the roots after flowering (Fig. 3).

To further evaluate the spatial distribution of As, the ratios of As contents between two neighboring tissues were calculated using the data for 76 DAT (Fig. 4). The lowest As content ratio (0.08) was found for the ratio of the As content of leaf 3 to that of the roots. The ratios for the pairs leaf 2:leaf 3, leaf 1:leaf 2, and internode 1:internode 2 were 0.59, 0.68 and 0.62, respectively. By contrast, the ratio of the As content of the panicle (including the caryopsis, grain and pedicel) to that of leaf 1 was close to unity (1.12).

Arsenic speciation

In order to estimate the contributions of As species to the accumulation of As in the grain, As species were measured by HPLC-ICP-MS. Because As(III) was the main species found in the xylem sap of rice (Zhao *et al.*, 2009) and there was the potential for oxidation of As(III) during the extraction procedure, As(III) and As(V) were reported together as inorganic As (As_i) in this study. As_i was the predominant As species in the root, leaf and stem, accounting for 90.5–97.1% of the total As, whereas reproductive tissues contained substantially higher proportions of DMA than

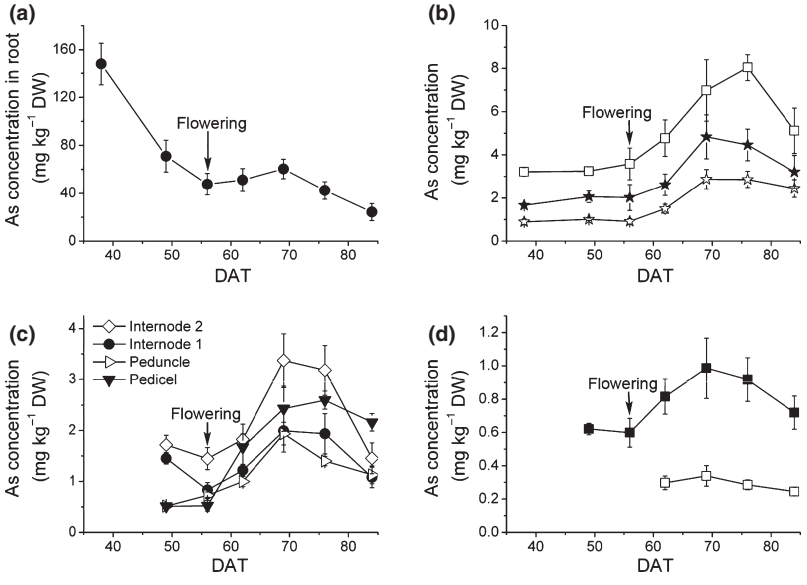

Fig. 2 Variation in the total arsenic (As) concentration in the roots and aerial tissues of rice (*Oryza sativa*) plants at different growth stages (days after transplant (DAT)). Data are the mean ± SE (n = 4).

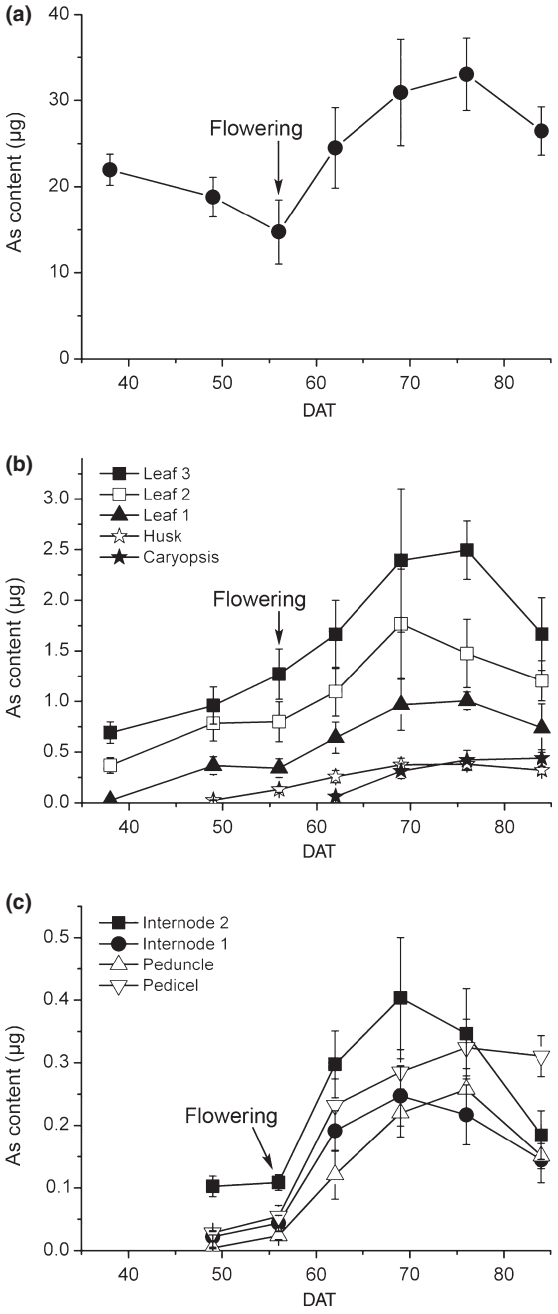

Fig. 3 Variation in the arsenic (As) content in different tissues of rice (*Oryza sativa*) plants. Arsenic contents were calculated by multiplying biomass by As concentration. (a) The As content in the root. Note the sharp increase after flowering. (b, c) The As contents in various tissues of the main tiller. Data are the mean ± SE (n = 4). DAT, days after transplant.

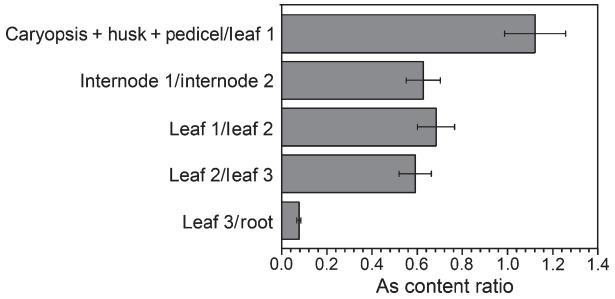

Fig. 4 Ratios of arsenic (As) content between two neighbouring tissues of rice (*Oryza sativa*) plants at 76 days after transplant (DAT). Data are the mean ± SE (n = 4).

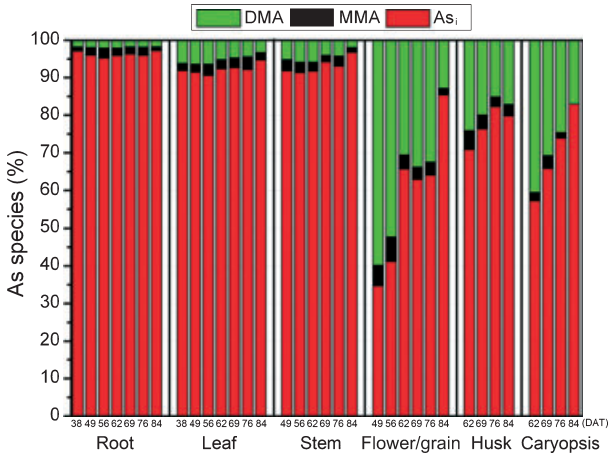

Fig. 5 Temporal variation in the percentages of arsenic (As) species in different tissues of rice (*Oryza sativa*) plants. Arsenic species were quantified using high-performance liquid chromatography–inductively coupled plasma mass spectroscopy (HPLC-ICP-MS) and the mean values obtained from three replicates are presented. DMA, dimethylarsinic acid; MMA, monomethylarsonic acid; As_i, inorganic As.

the vegetative tissues (Fig. 5). In flowers and grains, the percentage of DMA decreased significantly from 59.8% at 49 DAT to 12.9% at 84 DAT. A similar trend was found in the caryopsis, where the percentage of DMA decreased from 40.5% at 69 DAT to 24.6% at 84 DAT (Fig. 5). While the concentration of DMA in the caryopsis decreased during grain filling (Fig. 6a), the total DMA content remained stable (Fig. 6b). By contrast, the concentration of As_i in the caryopsis remained stable during its development (Fig. 6c), while the total content of As_i increased (Fig. 6d). In this tissue the total As concentration decreased with DAT because of the decrease in the concentration of DMA (Fig. 6a,c). The total As concentrations in the roots, leaves, stems and husks showed the same patterns as As_i concentrations.

To compare the translocation efficiency among different As species, the caryopsis-to-root concentration ratio was analyzed at 76 DAT. The highest translocation efficiency was found for DMA (0.088), followed by MMA (0.008) and As_i (0.004) (Fig. 7a). Interestingly, the order of translocation efficiency varied in different parts of the rice plant. From the husk to the caryopsis, the translocation efficiency for As_i, DMA and MMA was 0.24, 0.62 and 0.40, respectively (Fig. 7b). From the leaf to the husk, there was a large

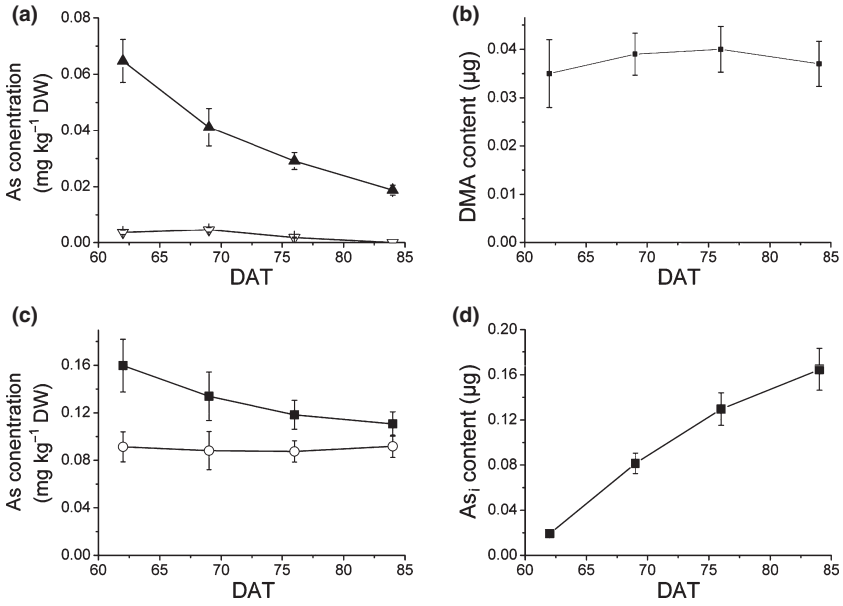

Fig. 6 Variation in arsenic (As) species in the rice (*Oryza sativa*) caryopsis during its development. Data are the mean ± SE (n = 4). DAT, days after transplant; DMA, dimethylarsinic acid; MMA, monomethylarsonic acid; As$_i$, inorganic As.

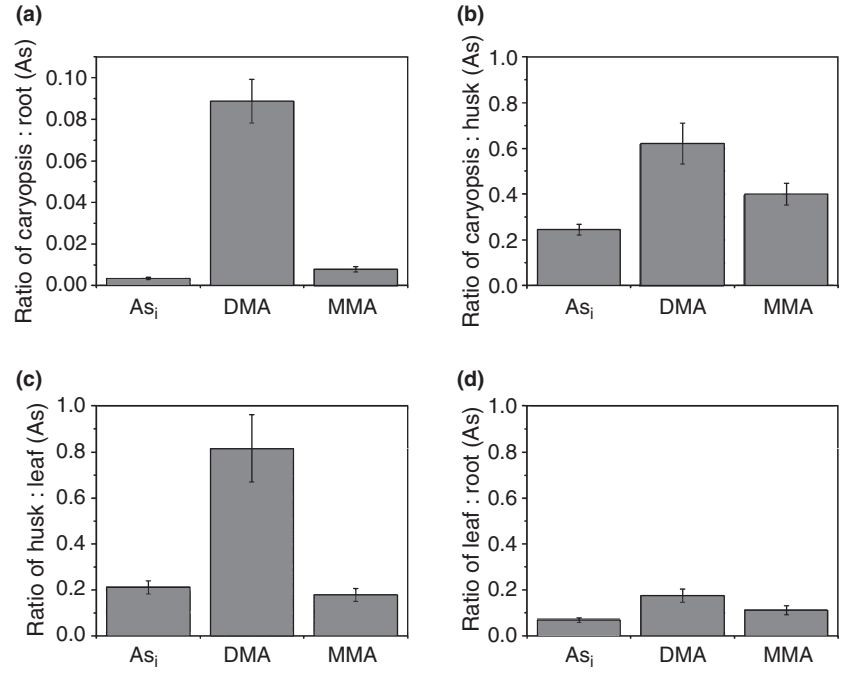

Fig. 7 The ratios of arsenic (As) content for rice (*Oryza sativa*) caryopsis : root (a), caryopsis : husk (b), husk : leaf (c), and leaf : root (d). DMA, dimethylarsinic acid; MMA, monomethylarsonic acid; As$_i$, inorganic As.

increase for DMA (0.82), and small decreases for MMA (0.18) and As$_i$ (0.21) (Fig. 7c). From the root to the leaf, translocation efficiencies for all As species were dramatically lower than those in other sites (Fig. 7d).

In situ As localization

In order to reveal As localization *in situ*, liquid nitrogen-frozen samples were used for SXRF scanning (the sampled material had the following dimensions: leaf, area 11 × 16 mm; internode, length 1.5 mm; node, length 2.0 mm; caryopsis, whole caryopsis). When considering the SXRF image data, it must be borne in mind that SXRF imaging compresses 3D information into 2D. We found that As localization was tissue-specific in the rice plant. In leaves, the As signal was detected mainly in the veins, especially the main veins (Fig. 8a,b). Similarly, As was found to be concentrated in the vascular system of stems, although

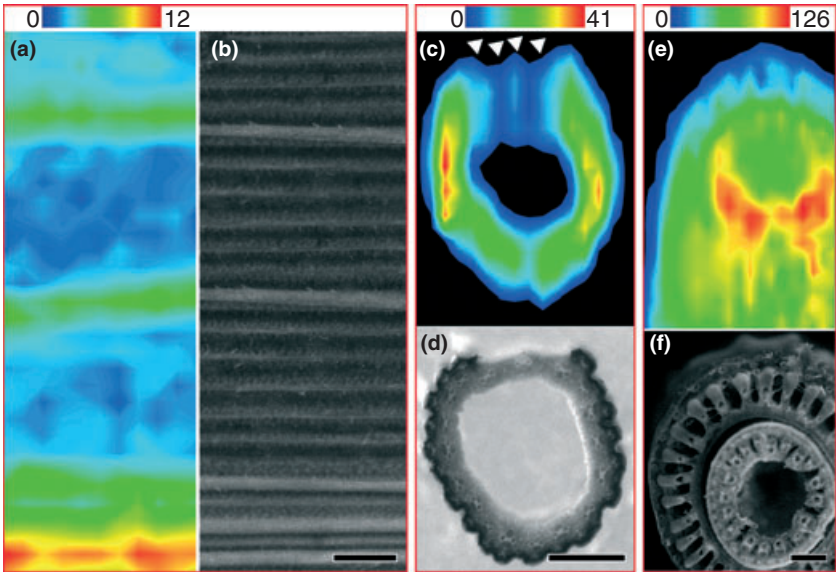

Fig. 8 Synchrotron X-ray fluorescence (SXRF) images of arsenic (As) distribution in the leaf, internode and node of rice (*Oryza sativa*) plants. The emission intensity of each pixel was normalized using the beam intensity as a reference. (a) A leaf section. Note that high As signals coincided with the veins shown in (b). (b) Light micrograph of the same leaf as in (a). (c) Cross-section of an internode. Note the absence of As signal at the side (indicated by an arrow) from which the leaf grew. (d) Light micrograph of the same internode as in (c). (e) Cross-section of a node, showing an intense As signal in the center. (f) Light micrograph of the same node as in (e). Bar, 500 μm.

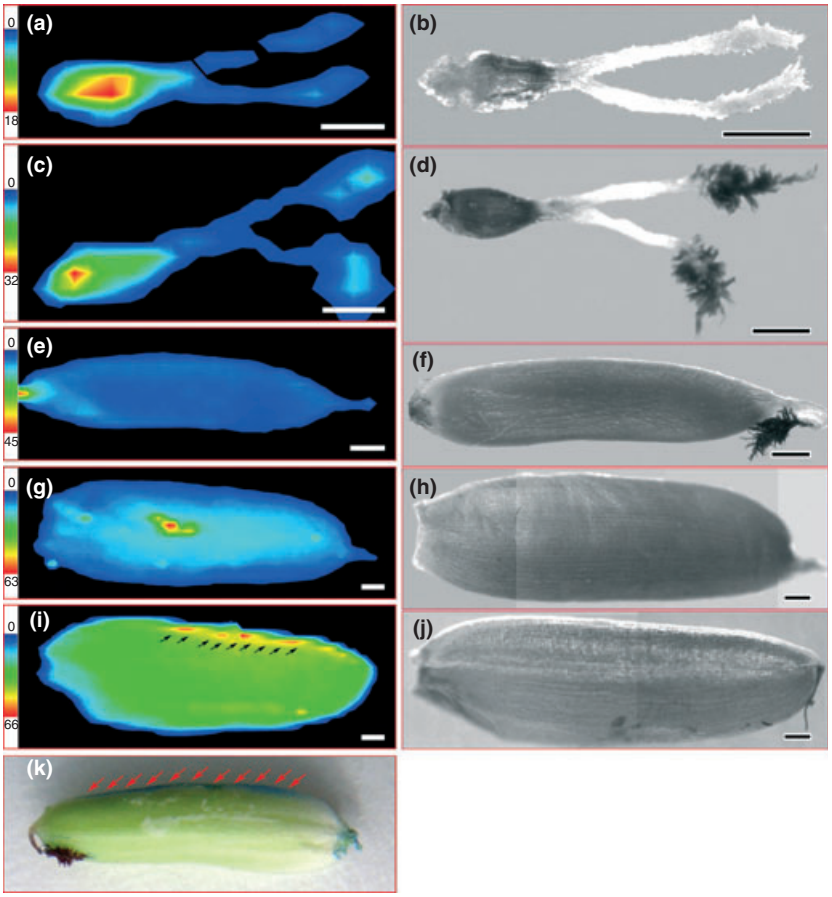

Fig. 9 Synchrotron X-ray fluorescence (SXRF) images of arsenic (As) distribution in rice (*Oryza sativa*) caryopses at different developmental stages. The emission intensity of each pixel was normalized using the beam intensity as reference. (a) A pistil at 3 d before flowering (53 days after transplant (DAT)). Note the abundant As localized in the center of the ovary. (b) Light micrograph of the same pistil as in (a). (c) A pistil on the day of flowering, showing a similar As distribution pattern as that in (a), but the As-intense area had shrunk. (d) Light micrograph of the same pistil as in (c). (e) A caryopsis at 4 d after flowering (DAF). Note the accumulation of As signal in the chalazal tissue. (f) A light micrograph of the same caryopsis as in (e). (g) A caryopsis at 14 DAF, showing a diffuse As distribution. (h) A light micrograph of the same caryopsis as in (g). (i) A ripened caryopsis (32 DAF). Note the overall relatively high As signal in the whole caryopsis and an accumulation of As along the ovular vascular trace (arrow). (j) A light micrograph of the same caryopsis as in (i). (k) A rice caryopsis dyed with aniline blue shows the localization of the ovular vascular trace (blue color, indicated by arrows). Bar, 500 μm.

the As signal was absent from the side on which the leaf grew (Fig. 8c,d), suggesting that As was transported into the leaf. An intense As signal was observed in the center of the node below the peduncle (Fig. 8e,f).

Arsenic localization in the caryopsis was time-dependent. At 3 d before flowering (53 DAT), strong As signals were observed in the center of the ovary (Fig. 9a,b). With the development of the ovary, this intense As signal disappeared

progressively from the center and appeared at the base of the caryopsis (Fig. 9c–f). At 14 DAF, an obvious As signal was found at the central point (Fig. 9g,h).When grain filling had finished, an additional As signal was observed in the region associated with the ovular vascular trace at the ventral side of the caryopsis (Fig. 9i–k).

Discussion

Arsenic contents in the various tissues of the rice plant change with growth stage and environmental conditions. It was previously reported that aerobic treatment for 3 wk before and after heading was most effective in reducing the As concentration in the grain (Arao *et al.*, 2009). In the present study, we found that DMA was the predominant As form in flowers before flowering and its concentration decreased progressively with the development of the caryopsis. This decrease in concentration was probably caused by dilution because the total content of DMA in the caryopsis remained constant throughout grain filling. These results suggest that DMA was transported into and accumulated in the ovary before fertilization. To date it has not been resolved whether rice plants obtain DMA from the soil or are able to methylate As_i *in planta* (Zhao *et al.*, 2010). The high ratio of DMA in the caryopsis to that in the root suggests efficient translocation, which may explain the abundant accumulation of DMA in the ovary before flowering if DMA is taken up by roots from the soil. Moreover, given that rice plants grown under flooded conditions contained much more DMA in the grain than aerobically grown rice plants (Xu *et al.*, 2008; Li *et al.*, 2009), introducing a period of aerobic conditions in the soil before fertilization may decrease the DMA concentration in the grain.

By contrast, As_i concentration remained stable in the caryopsis and As_i content increased with increasing biomass of the caryopsis, suggesting that unloading of As_i into the caryopsis was concomitant with carbohydrate accumulation during grain filling. Furthermore, there were increases in As concentration in the leaves and internodes during the first 2 wk after flowering. Given that As_i comprised 90.5–97.3% of the total As in vegetative tissues and that variation in total As concentration coincided with variation in As_i in these tissues, the increase in total As concentration in vegetative tissues suggested that the first 2 wk after flowering is a key period affecting As_i accumulation in the grain. In agreement with this, Arao *et al.* (2009) reported that flooding after heading produced a greater increase in As_i concentration than flooding before heading. In a recent study using stem girdling of excised panicles, Carey *et al.* (2010) estimated that phloem transport accounted for 90% and 55% of As(III) and DMA, respectively, in the caryopsis. The phloem-mediated transport of As(III) to the rice grain is consistent with our observation that the unloading of As_i into the caryopsis correlated closely with carbohydrate accumulation.

Arsenic uptake by roots is the initial source of As in the grain. In this study, over 55% of the As present was found in the roots, indicating restricted translocation of As from roots to shoots. This phenomenon has been well documented, and is probably a result of the sequestration of As(III)–thiol complexes in the vacuole in roots (Bleeker *et al.*, 2006; Zhao *et al.*, 2009). Additionally, loading of As into the xylem may be limited. Recently, Ma *et al.* (2008) showed that Lsi2 localized to the proximal side of the exodermis and endodermis of rice roots plays a key role in controlling As translocation to the shoots.

In the above-ground tissues, the total As concentration decreased from the basal leaf and stem internode to the upper leaf and panicle. This pattern suggests that there are additional check-points along the stem. At rice nodes, there are large and small vascular bundles and diffuse vascular bundles. Large and small vascular bundles originating from the lower nodes connect to the leaf that grows at the basal section of the node; these vascular bundles are markedly enlarged at the node. Diffuse vascular bundles are linked to large vascular bundles via nodal vascular anastomoses in the basal region of the node, and are then assembled in the upper internode (or panicle) to form regular bundles (Kawahara *et al.*, 1974; Chonan *et al.*, 1985). This pattern suggests that nodes may control the flow of As towards the leaf or upper internode. This hypothesis is supported by the SRXF data showing high As signals in the node and the absence of an As signal in the side of the internode where the leaf grew. Furthermore, it was also found that the ratios of As content between neighboring leaves or between neighboring internodes were *c.* 0.6, suggesting that the node distributed *c.* 40% of the As from the lower node to the closest sink (leaf) and the other 60% to the upper portion of the shoot. Furthermore, the ratio of As content in the panicle to that in leaf 1 was near unity, because there are no more leaves on the peduncle. Recently, Yamaji & Ma (2009) reported that Lsi6 localized in rice nodes is responsible for intervascular transfer of Si from the large vascular bundle to the diffuse vascular bundle, and thus regulates the distribution of Si to leaves or panicles. Lsi6 was previously shown to be permeable to arsenite when the gene was expressed in *Xenopus laevis* oocytes (Ma *et al.*, 2008). Whether this transporter is involved in As distribution in the node remains unknown. Norton *et al.* (2010b) examined As speciation in the shoot and grains at maturity in a wide range of cultivars and found that the higher the shoot As concentration, the lower the proportion (but not the amount) of As that reaches the grain. It is possible that differences among cultivars may partly be explained by the control exerted by the node.

In summary, our investigation has, for the first time, documented in detail the spatial distribution and temporal

variation of As in the whole rice plant, providing a more global view of the transport of As into grains. The study revealed that DMA had already accumulated in flowers before fertilization, whereas As_i was unloaded into the grain concomitant with carbohydrate accumulation after fertilization. In addition, our results show that nodes are likely to serve as an important check-point in As transport upward from the root to the grain.

Acknowledgements

This work was supported by the Natural Science Foundation of China (20720102042) and the Ministry of Science and Technology (2009DFB90120). We thank the Shanghai Institute of Applied Physics, Chinese Academy of Science, for providing technical support in relation to the synchrotron X-ray fluorescent microprobe. F-J.Z. is supported by the CAS/SAFEA International Partnership Program for Creative Research Teams (KZCX2-Yw-T08).

References

Abedin MJ, Cresser MS, Meharg AA, Feldmann J, Cotter-Howells J. 2002. Arsenic accumulation and metabolism in rice (*Oryza sativa* L.). *Environmental Science and Technology* **36**: 962–968.

Arao T, Kawasaki A, Baba K, Mori S, Matsumoto S. 2009. Effects of water management on cadmium and arsenic accumulation and dimethylarsinic acid concentrations in Japanese rice. *Environmental Science and Technology* **43**: 9361–9367.

Bhattacharjee Y. 2007. Toxicology. A sluggish response to humanity's biggest mass poisoning. *Science* **315**: 1659–1661.

Bleeker PM, Hakvoort HW, Bliek M, Souer E, Schat H. 2006. Enhanced arsenate reduction by a CDC25-like tyrosine phosphatase explains increased phytochelatin accumulation in arsenate-tolerant *Holcus lanatus*. *Plant Journal* **45**: 917–929.

Carey AM, Scheckel KG, Lombi E, Newville M, Choi Y, Norton GJ, Charnock JM, Feldmann J, Price AH, Meharg AA. 2010. Grain unloading of arsenic species in rice (*Oryza sativa* L.). *Plant Physiology* **152**: 309–319.

Chen Z, Zhu Y-G, Liu W-J, Meharg AA. 2005. Direct evidence showing the effect of root surface iron plaque on arsenite and arsenate uptake into rice (*Oryza sativa*) roots. *New Phytologist* **165**: 91–97.

Chonan N, Kawahara H, Matsuda T. 1985. Ultrastructure of elliptical and diffuse bundles in the vegetative nodes of rice. *Nihon Sakumotsu Gakkai Kiji* **54**: 393–402.

Duan GL, Zhu YG, Tong YP, Cai C, Kneer R. 2005. Characterization of arsenate reductase in the extract of roots and fronds of Chinese brake fern, an arsenic hyperaccumulator. *Plant Physiology* **138**: 461–469.

Kawahara H, Chonan N, Matsuda T. 1974. Studies on morphogenesis in rice plants 7. The morphology of vascular bundles in the vegetative nodes of the culm. *Nihon Sakumotsu Gakkai Kiji* **43**: 389–401.

Kile ML, Houseman EA, Breton CV, Smith T, Quamruzzaman Q, Rahman M, Mahiuddin G, Christiani DC. 2007. Dietary arsenic exposure in Bangladesh. *Environmental Health Perspectives* **115**: 889–893.

Krishnan S, Dayanandan P. 2003. Structural and histochemical studies on grain-filling in the caryopsis of rice (*Oryza sativa* L.). *Journal of Biosciences* **28**: 455–469.

Li RY, Ago Y, Liu WJ, Mitani N, Feldmann J, McGrath SP, Ma JF, Zhao FJ. 2009. The rice aquaporin Lsi1 mediates uptake of methylated arsenic species. *Plant Physiology* **150**: 2071–2080.

Liao XY, Chen TB, Xie H, Liu YR. 2005. Soil As contamination and its risk assessment in areas near the industrial districts of Chenzhou City, Southern China. *Environment International* **31**: 791–798.

Liu WJ, Wood BA, Raab A, McGrath SP, Zhao FJ, Feldmann J. 2010. Complexation of arsenite with phytochelatins reduces arsenite efflux and translocation from roots to shoots in *Arabidopsis thaliana*. *Plant Physiology* **152**: 2211–2221.

Ma JF, Yamaji N, Mitani N, Xu XY, Su YH, McGrath SP, Zhao FJ. 2008. Transporters of arsenite in rice and their role in arsenic accumulation in rice grain. *Proceedings of the National Academy of Sciences, USA* **105**: 9931–9935.

Meharg AA, Lombi E, Williams PN, Scheckel KG, Feldmann J, Raab A, Zhu Y, Islam R. 2008. Speciation and localization of arsenic in white and brown rice grains. *Environmental Science and Technology* **42**: 1051–1057.

Meharg AA, Rahman MM. 2003. Arsenic contamination of Bangladesh paddy field soils: implications for rice contribution to arsenic consumption. *Environmental Science and Technology* **37**: 229–234.

Mondal D, Polya DA. 2008. Rice is a major exposure route for arsenic in Chakadaha block, Nadia district, West Bengal, India: a probabilistic risk assessment. *Applied Geochemistry* **23**: 2987–2998.

Norton GJ, Duan G, Dasgupta T, Islam MR, Lei M, Zhu Y, Deacon CM, Moran AC, Islam S, Zhao FJ *et al.* 2010a. Environmental and genetic control of arsenic accumulation and speciation in rice grain: comparing a range of common cultivars grown in contaminated sites across Bangladesh, China, and India. *Environmental Science and Technology* **43**: 8381–8386.

Norton GJ, Islam MR, Duan G, Lei M, Zhu Y, Deacon CM, Moran AC, Islam S, Zhao FJ, Stroud JL *et al.* 2010b. Arsenic shoot-grain relationships in field grown rice cultivars. *Environmental Science and Technology* **44**: 1471–1477.

Ohno K, Yanaase T, Matsuo Y, Kimura T, Rahman MH, Magara Y, Matsui Y. 2007. Arsenic intake via water and food by a population living in an arsenic-affected area of Bangladesh. *Science of the Total Environment* **381**: 68–76.

Smith AH, Lopipero PA, Bates MN, Steinmaus CM. 2002. Public health. Arsenic epidemiology and drinking water standards. *Science* **296**: 2145–2146.

Sun GX, Williams PN, Carey AM, Zhu YG, Deacon C, Raab A, Feldmann J, Islam RM, Meharg AA. 2008. Inorganic arsenic in rice bran and its products are an order of magnitude higher than in bulk grain. *Environmental Science and Technology* **42**: 7542–7546.

Williams PN, Islam MR, Adomako EE, Raab A, Hossain SA, Zhu YG, Feldmann J, Meharg AA. 2006. Increase in rice grain arsenic for regions of Bangladesh irrigating paddies with elevated arsenic in groundwaters. *Environmental Science and Technology* **40**: 4903–4908.

Williams PN, Lei M, Sun G, Huang Q, Lu Y, Deacon C, Meharg AA, Zhu YG. 2009. Occurrence and partitioning of cadmium, arsenic and lead in mine impacted paddy rice: Hunan, China. *Environmental Science and Technology* **43**: 637–642.

Williams PN, Price AH, Raab A, Hossain SA, Feldmann J, Meharg AA. 2005. Variation in arsenic speciation and concentration in paddy rice related to dietary exposure. *Environmental Science and Technology* **39**: 5531–5540.

Williams PN, Raab A, Feldmann J, Meharg AA. 2007. Market basket survey shows elevated levels of As in South Central U.S. processed rice compared to California: consequences for human dietary exposure. *Environmental Science and Technology* **41**: 2178–2183.

Xu XY, McGrath SP, Meharg AA, Zhao FJ. 2008. Growing rice aerobically markedly decreases arsenic accumulation. *Environmental Science and Technology* **42**: 5574–5579.

Yamaji N, Ma JF. 2009. A transporter at the node responsible for intervascular transfer of silicon in rice. *The Plant Cell* **21**: 2878–2883.
Zhao FJ, Ma JF, Meharg AA, McGrath SP. 2009. Arsenic uptake and metabolism in plants. *New Phytologist* **181**: 777–794.
Zhao FJ, McGrath SP, Meharg AA. 2010. Arsenic as a food-chain contaminant: mechanisms of plant uptake and metabolism and mitigation strategies. *Annual Review of Plant Biology* **61**: 535–559.
Zhu YG, Sun GX, Lei M, Teng M, Liu YX, Chen NC, Wang LH, Carey AM, Deacon C, Raab A *et al.* 2008. High percentage inorganic arsenic content of mining impacted and nonimpacted Chinese rice. *Environmental Science and Technology* **42**: 5008–5013.

Supporting Information

Additional supporting information may be found in the online version of this article.

Fig. S1 Images showing the positions of samples collected for total arsenic (As) concentration analysis.

Fig. S2 Images showing the developmental stages of the whole rice plant (a), the flower (b) and caryopses (c).

Please note: Wiley-Blackwell are not responsible for the content or functionality of any supporting information supplied by the authors. Any queries (other than missing material) should be directed to the *New Phytologist* Central Office.